



The spectra of isotopic heterogeneities along the mid-Atlantic Ridge

Arnaud Agranier^a, Janne Blichert-Toft^{a,*}, David Graham^b, Vinciane Debaille^c,
Pierre Schiano^c, Francis Albarède^a

^a *Ecole Normale Supérieure, 69007 Lyon, France*

^b *Oregon State University, Corvallis OR 97331, USA*

^c *Laboratoire Magmas et Volcans, 63038 Clermont-Ferrand, France*

Received 28 March 2005; received in revised form 2 July 2005; accepted 4 July 2005

Available online 18 August 2005

Editor: R.D. van der Hilst

Abstract

Due to the advent of large-throughput plasma source mass spectrometers, extensive sets of high-precision Pb, Nd, and Hf isotopic data can now be produced on mid-ocean ridge basalts. A first such set of isotopic results on the mid-Atlantic Ridge is examined here in combination with literature data. The spectra of the data vs. latitude are strongly colored. When combined with conventional scatter plots, they reveal two contrasting types of behavior. The signal of the Icelandic hot spot is clearly identifiable on the spectra of $^{206}\text{Pb}/^{204}\text{Pb}$, $^{207}\text{Pb}/^{204}\text{Pb}$, $^{208}\text{Pb}/^{204}\text{Pb}$, the first principal component of Pb isotopes, $^{87}\text{Sr}/^{86}\text{Sr}$, and $^3\text{He}/^4\text{He}$, over length scales of 6–10° (type A spectrum). In contrast, the power decreases in a near-continuous manner for the isotopic signals of Nd and Hf, and for the second Pb isotope principal component (type B spectrum). We interpret type B spectra as a dynamic cascade, in which the size of mantle heterogeneities is continually reduced upon stretching and refolding of the mantle by convection. The power law coefficient of this spectrum has an exponent of -1 indicative of a Batchelor regime and reflects a smooth, but chaotic, probably steady-state flow. Since the isotopic properties of the type B spectra also characterize the EM I+EM II mix of the Dupal anomaly, we infer that they depict the convective northward dispersal ('reeling off') of the Southern Hemisphere anomalous mantle.

© 2005 Elsevier B.V. All rights reserved.

Keywords: mid-Atlantic Ridge; MORB; Hf isotopes; Pb isotopes; mantle heterogeneities; mixing; DUPAL; periodograms

1. Introduction

Because basalts erupted along mid-ocean ridges (MORB) tap the asthenospheric mantle almost continuously over 50,000 km, their geochemical properties offer a unique representation of the history of a

* Corresponding author.

E-mail address: jblicher@ens-lyon.fr (J. Blichert-Toft).

very large fraction of the upper mantle. Although the overall petrological properties of MORB provide some insight into the melting processes taking place beneath ridges [1], it is clear from the range of isotopic compositions of these basalts that the evolution of their mantle source involves a series of various geodynamic events over variable lengths of time [2]. In other words, the asthenospheric mantle is geochemically diverse. On a scale at which molecular diffusion can safely be neglected (>1 m), different sources of geochemical anomalies are recognized. First, the mantle may already have been heterogeneous initially, i.e., right after the Earth had accreted and began to differentiate, possibly through fractionation processes within a magma ocean. Primordial layering is to a large extent transient and its survival should be scaled by the number of convective cycles since the beginning of Earth's history. Second, the continuous injection of lithospheric plates processed by magmatic and metamorphic processes from ridge crests to subduction zones keep on introducing differentiated material into the mantle. Upon subduction, 5–10 km thick lithologic sequences typical of oceanic crust will be folded within much thicker layers of oceanic lithosphere and ambient mantle [3]. In contrast to the heterogeneities created by the primordial differentiation, those inherited from plate tectonics likely have been continually produced throughout the entire geological history and should be scaled by a much smaller number of convective cycles. With subduction velocities reaching several centimeters per year, it is inescapable that, once multiply stretched and refolded by mantle convection, old plates find their way back to the asthenospheric upper mantle, where they become an intrinsic part of the MORB source. In addition to crust segregation at ridge crests, other geodynamic processes, notably delamination of subcontinental lithosphere [4] and metasomatism at subduction zones, potentially act to create heterogeneities that mantle convection repeatedly folds and stretches. One would therefore expect that some striated character resulting from the complex processing of these geochemical heterogeneities, such as envisaged in the popular model of marble cake mantle [5,6], should be identifiable when well-located geochemical observations are made over long stretches of ridge crest.

Although the spectrum of isotopic mantle heterogeneities along mid-ocean ridges may simply be

inherited from the stretching and folding of heterogeneities imposed by mantle convection [7,8], it may also reflect overprinting of the mid-ocean ridges by blobs of deep mantle and hot spots [7,9]. Mapping mantle heterogeneities by using the isotope compositions of the daughter isotopes of long-lived systems, such as Sr, Nd, and Pb in MORB, hopefully should resolve the dilemma of a hot spot vs. stirring origin. So far, however, the task of producing enough high-precision isotopic data to observe significant short-wavelength variations along the mid-ocean ridge system has been daunting. The advent of multiple-collector inductively-coupled plasma mass spectrometry (MC-ICP-MS) recently changed this situation by allowing for much larger sample throughput than possible with conventional thermal ionization mass spectrometry. In addition, the improved quality of Pb isotopic data as produced by MC-ICP-MS enables better resolution of the small, but significant differences in Pb isotope space. Also, MC-ICP-MS has made it possible to explore Hf isotopes as efficiently as the other commonly used radiogenic isotopes. This work presents new MC-ICP-MS isotopic data for Hf and Pb, and when missing from the literature also Nd, on about half of >400 basalts from almost the entire mid-Atlantic Ridge (MAR), for which the Sr and most of the Nd isotope compositions were already known. The spectra of this new data set reveal two distinct behaviors for the respective isotopic tracers: a long-wavelength character best accounted for by the presence of mantle hot spots, and a pervasive shorter wavelength character best explained by the presence of asthenospheric mantle contaminated by ancient lithospheric plates that have been stretched and refolded by mantle convection.

2. Results and discussion

The analytical techniques used in this study have been described in detail elsewhere [10–13]. The in-run precisions of all the Pb, Hf, and Nd isotope data presented here are better than the external reproducibilities reported in these papers. The data are compiled in Table 1 (Appendix) and displayed in Fig. 1. The sample collection comprises a total of 426 MORB from 78°N to 55°S, of which new Pb, Hf, and Nd isotope data are presented for, respectively,

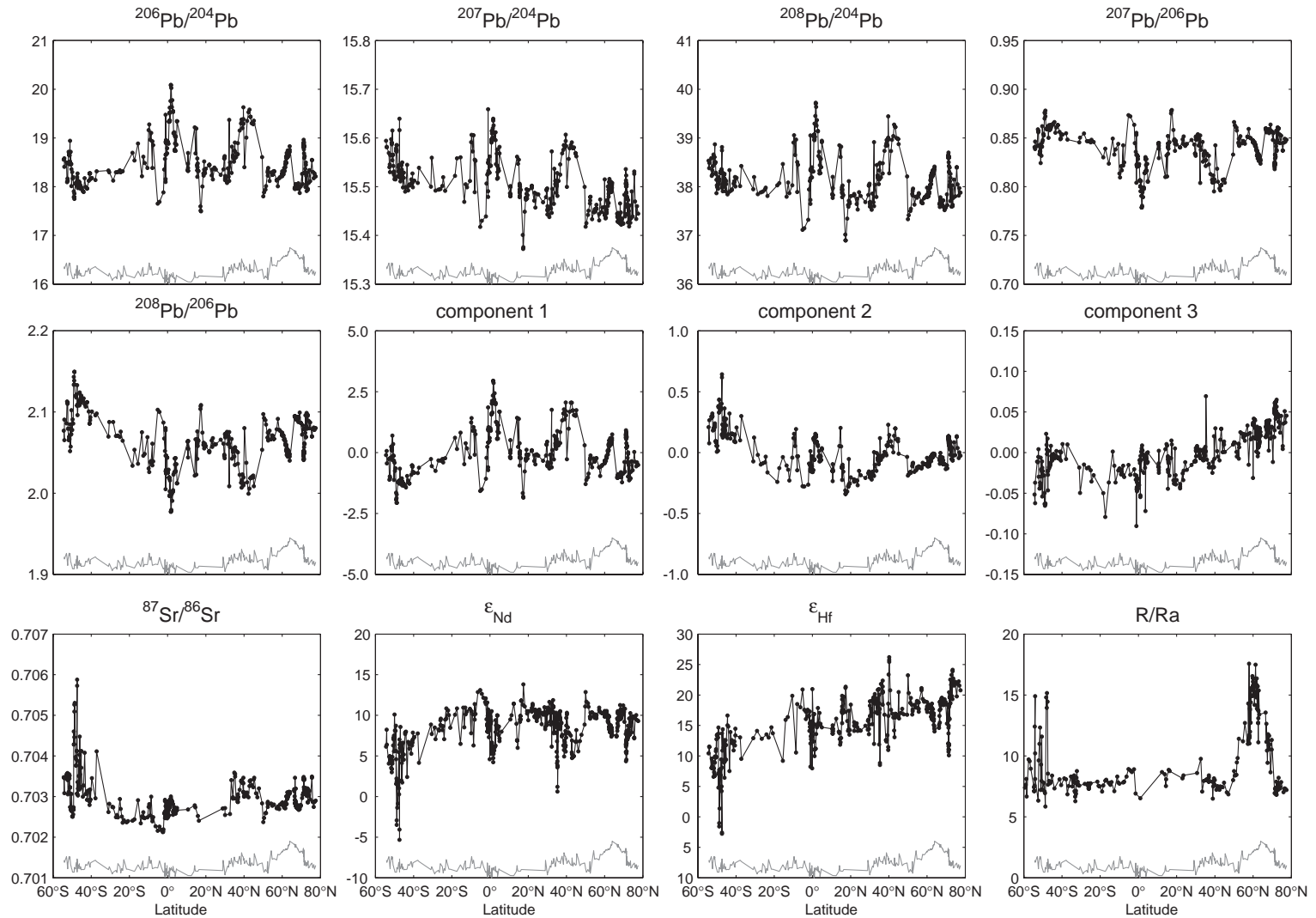


Fig. 1. Isotope data used in the present work viewed as a function of latitude along the mid-Atlantic Ridge. The Pb and Hf isotope data are either new or taken from recent projects carried out in Lyon. Sr, He, and most of the Nd isotope data are from the literature (see Table 1 in the Appendix for references). The $^3\text{He}/^4\text{He}$ data (presented as R/Ra, where Ra is the atmospheric ratio) were compiled by Graham [24]. The grey curves at the bottom of the diagrams show the bathymetry (~5000 mbsl to sea level). The first two Pb principal components account for 97.2 and 2.3%, respectively, of the total Pb isotope variability.

195, 140, and 9 samples. The rest of the data are published elsewhere, but all Pb and Hf isotope data are from our group and were acquired on the Lyon Plasma 54 over the past 5 yr. Due to lack of samples, there are no isotope data for the latitudes between 5 and 10°N and between 31 and 37°S. The consistency of our new data with the literature data compiled in the Lamont PETDB database and their improved quality is best illustrated by Pb isotopes when plotting both data sets together (Fig. 2). For $^{143}\text{Nd}/^{144}\text{Nd}$, the improvement in quality was not as substantial as for Pb isotopes and we therefore included Nd isotope data for 84 post-1987 basalt glasses downloaded from the PetDB data base.

2.1. Correlation structure

Although it is not the main purpose of the present work to break down into individual components the isotopic compositions of Atlantic MORB, which has been adequately dealt with by a number of authors, e.g., [12,14–17], it is nevertheless worthwhile highlighting some first-order features revealed by a quick examination of the multiple correlation plots (Fig. 3).

First, as argued elsewhere ([12] and Debaille et al. (submitted)), the dimensionality of the Pb isotopic space must be dealt with separately. Pb isotopic ratios usually show strong correlations because (1) the two parent nuclides ^{238}U and ^{235}U are isotopes of the same element, while the geochemical properties of Th are similar to those of U, and (2) a denominator common to all the ratios makes mixing relationships perfectly linear. It is therefore common practice [18] to calculate principal components of the Pb isotope distribution alone. The basis of Principal Component Analysis can be found in several standard textbooks (e.g., [19]). In order to make the analysis robust with respect to a change of units, we have adopted the components calculated from the correlation matrix. For the Atlantic MORB, the first two principal components account for, respectively, 97.2 and 2.3% of the Pb isotopic variability. For all practical purposes, the first component maps most of the $^{206}\text{Pb}/^{204}\text{Pb}$ variability, i.e., the abundance of the high U/Pb geochemical component in the mantle source. Blichert-Toft et al. [12] showed that the Pb isotope compositions of the most typical HIMU basalts [20] do not fall on a common alignment with North

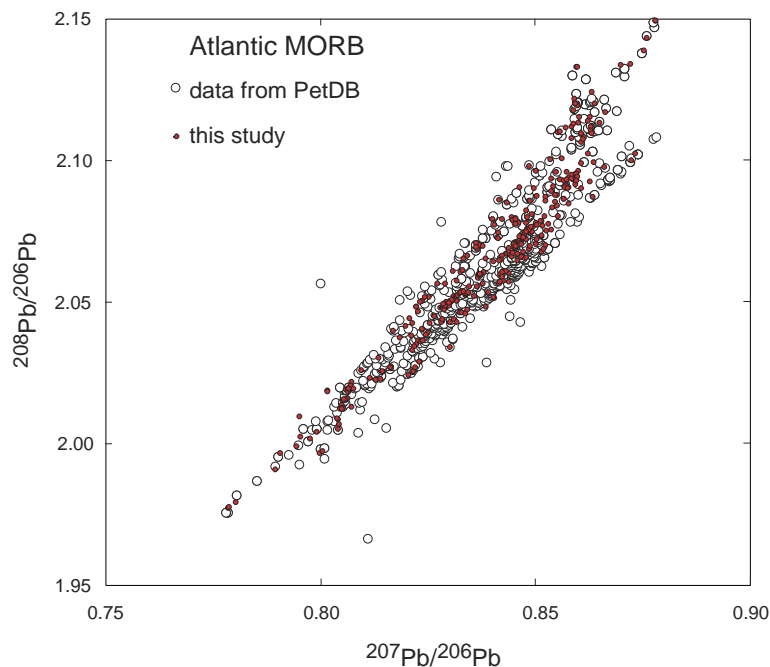


Fig. 2. Comparison of the dispersion of the present mid-Atlantic Ridge $^{207}\text{Pb}/^{206}\text{Pb}$ and $^{208}\text{Pb}/^{206}\text{Pb}$ data with the PETDB data from the same area. MC-ICP-MS techniques have visibly reduced the analytical noise.

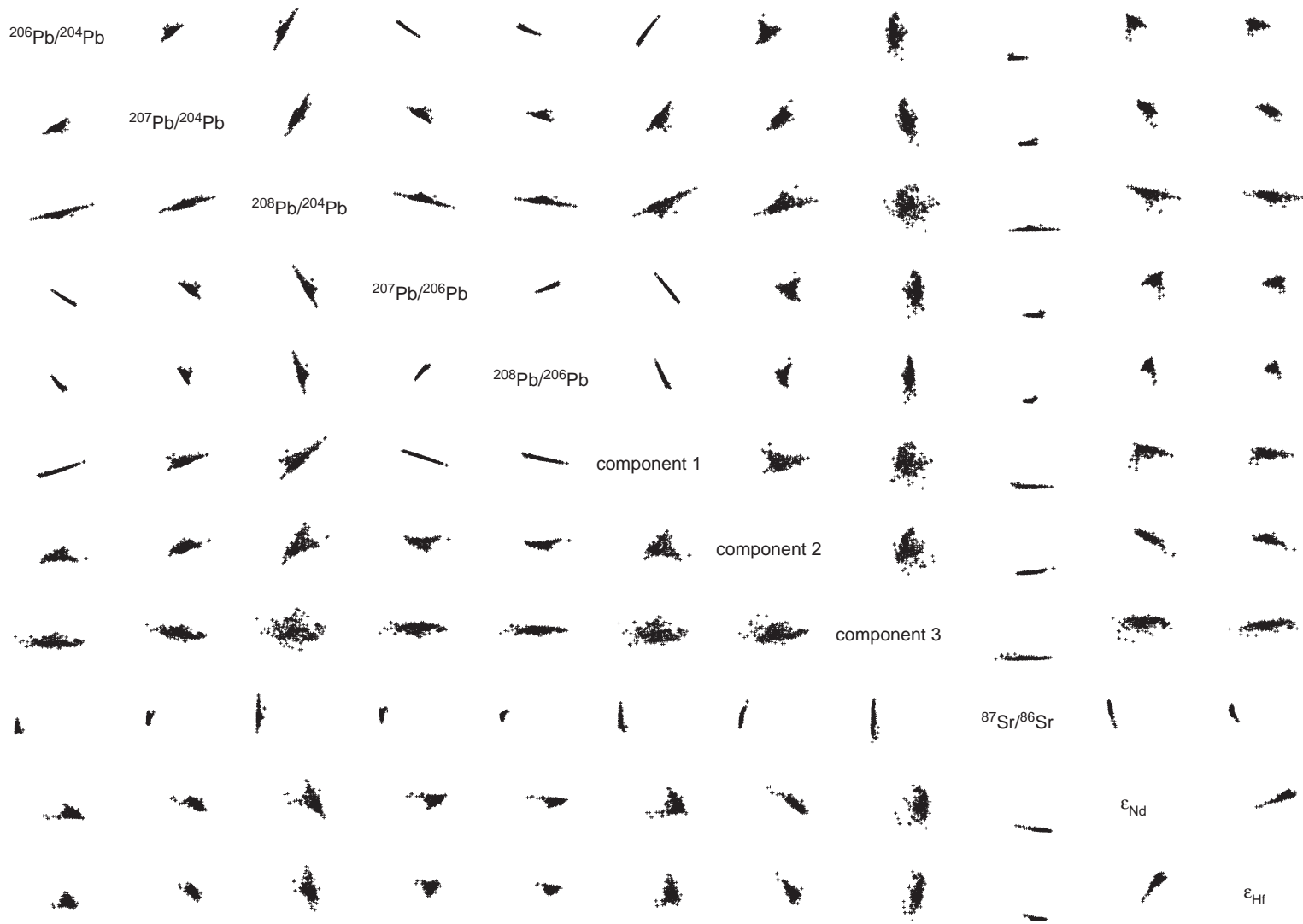


Fig. 3. Multiple correlation plots for MORB samples for which recent data are available. Components are principal components of the Pb isotopic data. The most noticeable correlations are observed between the first Pb principal component and the Pb isotopic ratios involving ^{204}Pb and also among ϵ_{Nd} , ϵ_{Hf} and the second Pb principal component.

Atlantic MORB and that the common component ‘C’ of Hanan and Graham [17] is a more suitable MORB end-member. The two geochemical components known as DM (depleted mantle) and ‘C’ form a nearly perfect mixing line and account for the well-known Northern Hemisphere Reference Line (NHRL) [21,22]. A small fraction of a third geochemical end-member (defined by the second Pb principal component), which can be identified as a mixture of the EM I and EM II ‘flavors’ (enriched mantle [20,23]), is needed for closure. We argue elsewhere ([12] and Debaille et al. (submitted)) that the third Pb principal component is essentially noise and make the case that only three geochemical end-members are needed to account for the total Pb isotopic variability on the mid-Atlantic Ridge.

Nearly binary correlations are observed between Nd and Hf isotope compositions and between Nd and the second Pb principal component (Fig. 3). The first Pb principal component is strongly correlated with every Pb isotope ratio involving ^{204}Pb . Most other correlation diagrams require at least ternary mixing and we will not repeat here the analysis already done elsewhere [20]. We finally note that, somewhat to our own surprise, we find that on a global scale, the correlation between isotopic ratios and bathymetry is extremely weak to nearly non-existent (see Fig. 1). A notable exception is Iceland. The general lack of high $^3\text{He}/^4\text{He}$ along the MAR, again except around Iceland and also at extreme southern latitudes around Shona and Discovery [24], suggests that the off-axis hot spots, such as the Azores and Cape Verde, are not associated with deep active upwelling.

2.2. Periodograms

Spectral techniques allow the efficient representation of a continuous, potentially complex property, such as the Nd isotope composition of basalts erupted at ridge axes, by a small number of discrete coefficients. For example, it only takes one coefficient to describe the shape of a sine wave distribution of ε_{Nd} along the ridge and it may take only a handful of them to describe the ‘hump’ defined by the anomalous isotopic ratios distributed about an isolated hot spot such as Iceland. In addition, since the power spectrum of a distribution is the Fourier transform of its autocorrelation function, spectral analysis captures

the characteristic length scales of geochemical heterogeneities. Finally, spectral techniques illuminate the physics of mixing processes: it is well established that, in chaotic flows, Lagrangian stretching or advective–diffusive transport are best characterized by the spectra of tracers transported in the flow field. Sampling, such as by dredging, coring, or recovery by submersible, or more subtly by melting processes, adds substantial complexity to the representation: a sampled function provides an incomplete spectrum usually limited by the sample distribution and density.

In order to extract spectra from large data sets, a common practice is to resort to Fast Fourier Transform (FFT) analysis, which provides an optimal set of independent parameters and can be computed through extremely efficient algorithms. However, this technique requires a complete record of equally spaced data, which is not the case for the present data set, where the density of observations varies considerably as a function of the spatial variable. Even if unequally spaced data could be handled by appropriate binning, the existence of two relatively broad gaps in our data set (between 5–10°N and 31–37°S) remains an issue. An additional limitation imposed by the independence of the spectrum coefficients is that FFT does not produce coefficients for very long wavelengths exceeding the size of the system (typically here the length of the ridge). We therefore opted for the Scargle periodogram [25,26], which is calculated by fitting sine functions of sample positions along the mid-Atlantic Ridge through the isotopic data. For a short and readily accessible reference, the reader may consult Section 13.8 of the *Numerical Recipes* of Press et al. [27]. For simplicity, let us consider the latitude θ as the position parameter and calculate the spectrum of a geochemical property y , which has been sampled at the positions $i=1, \dots, n$ defined by the numbers θ_1 to θ_n (e.g., $y_i = \varepsilon_{\text{Nd}}(\theta_i)$). The Scargle periodogram fits the observations y_i in such a way that the adjusted value \bar{y}_i satisfies:

$$\bar{y}_i = a \sin(2\pi k \theta_i + \varphi) + b \cos(2\pi k \theta_i + \varphi)$$

in which k is the wavenumber (the inverse of the wavelength), φ the phase, and a and b the unknown periodogram coefficients. For a given wavenumber k , a and b are found by minimizing the sum of squares $\sum_i (y_i - \bar{y}_i)^2$. The phase is simply eliminated by

shifting the origin of latitudes. Once properly normalized to the variance, the ‘power’ $P(k)=a^2+b^2$ is an exponentially distributed random variable, which allows a significance level to be defined for each k . The spectrum is obtained by plotting $P(k)$ with respect to the wavenumber k . A decisive advantage of the periodogram over other Fourier techniques is a minimal impact of aliasing with no nominal limitation at the Nyquist frequency (sampling density). Periodograms are also useful for testing the existence of periodic signals as peaks superimposed on an otherwise noisy background through a significance test on $P(k)$, which is exponentially distributed, and for the details of which the reader is referred to Press et al. [27].

The data set presented here was ‘tapered’ to minimize the leakage of the wavelengths generated by the finite sampling window (55°S–78°N) into the spectrum, which simply indicates that the data were multiplied by some bell-shaped function, which is unity almost everywhere except near each end, where it goes to zero. Various taper functions and ranges were tested with no appearance of significant differences.

Different position coordinates θ_i were considered for the present samples. We first looked at the latitude with respect to the Eulerian pole of opening. As predicted from the origin shift used to remove the dependence on φ , the spectra were similar to those obtained using straightforward geographic latitudes. Parameterizing the spatial distribution by the cumulative distances between successive samples using standard spherical trigonometry (e.g., [28], Section 1.8) is inadequate because irreducible gaps between consecutive ridge segments would appear along transform faults. We therefore chose to use the geographic latitudes as the position coordinates.

We also propagated the analytical uncertainties on the isotopic compositions into the periodogram and verified through Monte-Carlo experiments that the peak positions and intensities remained essentially identical. We further found that upon randomly removing 50% of the data, the spectra degraded some, but did not change their overall signature shape. Finally, we tested on relatively simple examples that the conventional spectrum obtained by FFT is correctly represented by the periodogram. A number of typical configurations were tested. Synthetic

examples show that even a broad sampling gap ($>10^\circ$) creates no spurious periodic effect and, as predicted by FFT theory, a broad anomaly, such as expected for a hot spot (e.g., Iceland), is readily identifiable as a large bulge in the power spectrum.

As a last consideration, we investigated the potential effect of melting on the spectrum and found none. Melts are produced over a finite ridge segment and collected in a magma chamber, thereby introducing some sort of moving average with a range and weights that depend on how MORB extraction is understood. On a relatively slow-spreading ridge, such as that of the Atlantic, the length of individual magma chambers is probably very short and we assume that the mean separation of 30 km between our samples is not seriously affected by this averaging process. In contrast, it is likely that MORB do not map mantle isotopic heterogeneities entirely faithfully, but we assume that there is no systematic bias introduced by melting. All the isotopic systems have a colored spectrum (Figs. 4 and 5). The ‘colored’ qualifier is used to make the distinction from a ‘white’ spectrum, which is characterized by a constant power across the entire range and signifies random distribution of uncorrelated anomalies at all length scales (i.e., noise). The present findings contrast with those of Gurnis [8], who concluded from a small set of Sr isotopic data that the power spectrum was essentially flat. Two clearly different types of spectra can be distinguished for our suite of samples:

- (i) *Type A*. For $^{206}\text{Pb}/^{204}\text{Pb}$, $^{207}\text{Pb}/^{204}\text{Pb}$, $^{208}\text{Pb}/^{204}\text{Pb}$, the first principal component of Pb isotopes, $^{87}\text{Sr}/^{86}\text{Sr}$, and $^3\text{He}/^4\text{He}$, there is a two-order-of-magnitude drop of the power at $k\sim 0.2/\text{degree}$. At wavelengths in excess of 550 km ($k<0.2/\text{degree}$), the spectra of these variables show peaks exceeding the 95% confidence level ($P(k)\sim 9.5$), as well as well-defined lobes with overtones most visible for $^3\text{He}/^4\text{He}$. Such lobes reflect the existence of a hump in an isotopic property vs. latitude plot, and for the present data set, this feature can be identified with the Iceland hot spot. The width of the He lobes is particularly narrow, which indicates that the high- $^3\text{He}/^4\text{He}$ halo around Iceland is *broader* than the width of the isotopic anomalies for Pb and Sr [29].

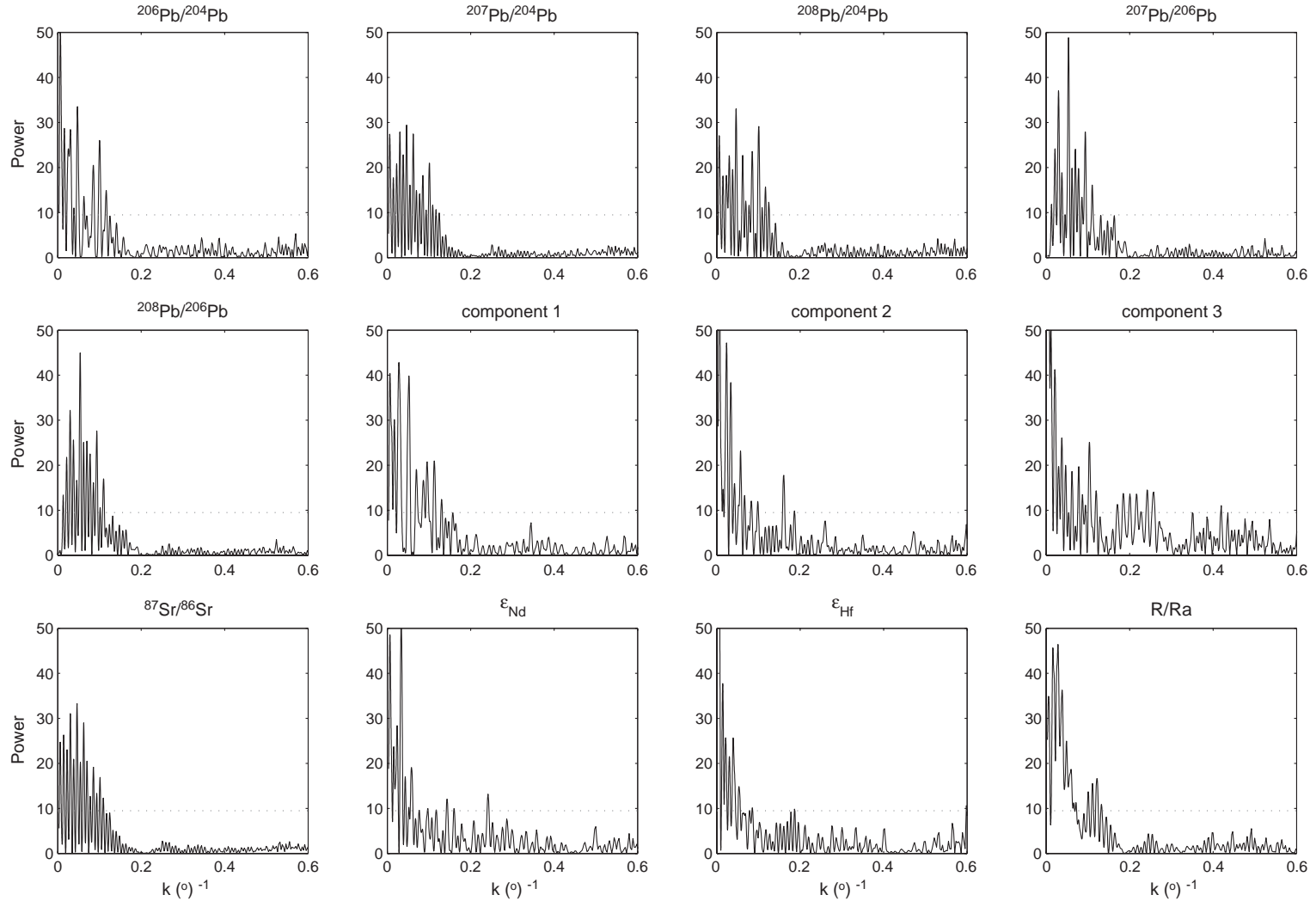


Fig. 4. Scargle periodograms of Pb, Sr, Nd, Hf, and He isotope compositions and the Pb principal components (linear scale). The horizontal scale is the wavenumber k , i.e., the reciprocal of the wavelength in degrees of latitude, while the vertical scale indicates the dimensionless power (square of the standard-deviation-normalized amplitudes). The ${}^3\text{He}/{}^4\text{He}$ spectrum (bottom right) is characteristic of hot spot-dominated anomalies (see Fig. 1) with well-defined lobes at low wavenumbers (long range) and white noise at large wavenumbers. The ${}^{207}\text{Pb}/{}^{204}\text{Pb}$, ${}^{208}\text{Pb}/{}^{206}\text{Pb}$, and ${}^{87}\text{Sr}/{}^{86}\text{Sr}$ spectra are similar to the ${}^3\text{He}/{}^4\text{He}$ spectrum. The power (~ 10) at the 95% confidence level for peaks is shown as a horizontal dotted line.

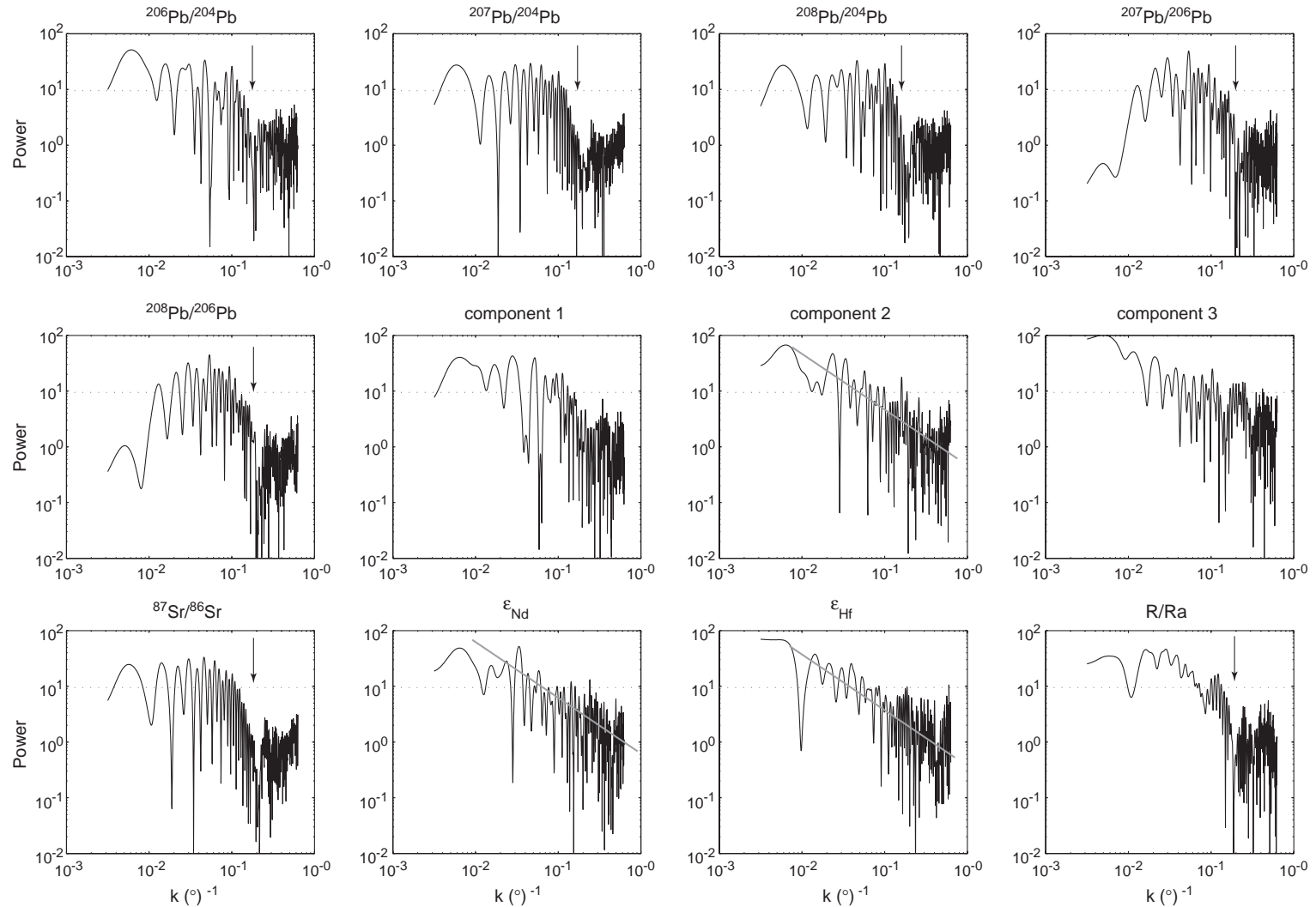


Fig. 5. Scargle periodograms of Pb, Sr, Nd, Hf, and He isotope compositions and the Pb principal components (log scale). Two contrasting types of spectra can be distinguished: (1) the ‘hot spot’ type A spectrum, epitomized by the $^3\text{He}/^4\text{He}$ spectrum (bottom right), with well-defined lobes at low k and a discontinuity at $k \sim 0.2$ (down-pointing arrow), and (2) the ‘cascade’ type B spectrum, in which the power steadily decreases with k . The slope of -1 (gray line) is indicative of a Batchelor regime, and reflects a smooth, but chaotic, probably steady-state flow field [38]. The cascade type B applies to $^{143}\text{Nd}/^{144}\text{Nd}$, $^{176}\text{Hf}/^{177}\text{Hf}$, and the second Pb principal component, which are characteristic of the Dupal (EM I+EM II) anomaly.

- (ii) *Type B*. In contrast, the spectra of $^{143}\text{Nd}/^{144}\text{Nd}$, $^{176}\text{Hf}/^{177}\text{Hf}$, and the second Pb principal component display a rather regular negative slope in the $\ln P$ vs. $\ln k$ plot. No significant peak emerges for $k > 0.2 \text{ degree}^{-1}$.

A similar contrast between the same variables is clearly visible in the position of the significant peaks in the long-wavelength part of the spectrum (Fig. 6).

The origin of isotopic heterogeneities beneath the mid-Atlantic Ridge. The spectra of the observed geochemical anomalies may arise from a number of different geodynamic conditions:

1. Mantle convection stretches and refolds lithospheric plates over geological time, thereby decreasing its characteristic length scale through time [6,30,31]. This is the essence of the marble cake model of Allègre and Turcotte [5]. Geochemical anomalies created by metasomatism in the mantle wedge above subduction zones or by delamination of the subcontinental lithosphere would appear similarly refolded.
2. The mid-Atlantic Ridge is delineated by abundant hot spots, notably Jan Mayen, Iceland, the Azores, Cape Verde, St. Helena, Tristan, Discovery, and Shona, which are all variously related to groups of islands, seamounts, or geochemically anomalous segments that may hint at elusive hot spots [15].
3. Mantle heterogeneities can be created by two-step melting under either dry [32] or wet [33] conditions above the transition zone. We contend, how-

ever, that these models do not account properly for either the strongly bimodal geochemical properties of oceanic basalts (MORB vs. OIB) or the apparent time scales of some of the isotopic heterogeneities recorded in MORB, especially the ca. 1.5 Ga slope of the NHRL [21,22]. We therefore will not discuss them further here.

4. Contamination of the upper mantle by delamination or rafting of subcontinental lithospheric mantle or lower crust may have occurred [34].

The long-wavelength part of the spectra of $^{206}\text{Pb}/^{204}\text{Pb}$, $^{207}\text{Pb}/^{204}\text{Pb}$, $^{208}\text{Pb}/^{204}\text{Pb}$, the first Pb principal component, $^{87}\text{Sr}/^{86}\text{Sr}$, and $^3\text{He}/^4\text{He}$ (type A) confirms that some of the geochemical anomalies are due to the presence of hot spots, first and foremost those of Iceland, Shona, and Discovery. The white character of these spectra at short wavelengths again suggests that these hot spots are the only ones to be associated with deep active upwelling along the MAR, which reflects that Cape Verde and the Azores currently are located some distance away from the ridge and do not contribute much to the local MORB compositions.

In contrast, we propose that the type B spectra ($^{43}\text{Nd}/^{144}\text{Nd}$, $^{176}\text{Hf}/^{177}\text{Hf}$, and the second Pb principal component) are unrelated to hot spots. Different arguments concur against assigning the bulk of the isotopic variability along the ridge to ridge-hot spot interaction: (i) the East Pacific Rise shows essentially no bathymetric highs that qualify as hot spots but still exhibits substantial broad-scale isotopic variability [35]. (ii) The histograms of isotopic ratios remain strongly unimodal along the mid-Atlantic Ridge (Fig. 7). Unimodality is not a simple effect of mixing since the prominent along-ridge geochemical variability would also be lost in the process and a white noise spectrum would ensue. (iii) Many of the geochemical anomalies do not seem to be associated with a bathymetric high (see Fig. 1).

‘Power law’-type spectra similar to type B are reasonably well explained by heterogeneity reduction in a chaotic flow. The geochemical heterogeneities subducted as oceanic crust and lithospheric mantle are stretched and refolded by convection, which therefore continuously reduces their size and strength: a time can always be found after which lithospheric material is reduced to pieces small enough that differ-

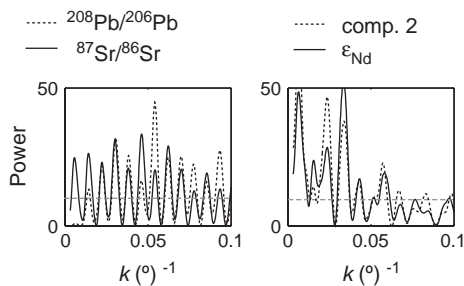


Fig. 6. Spectra superposition in the long-wavelength range. Both type A spectra, such as $^{87}\text{Sr}/^{86}\text{Sr}$ and $^{208}\text{Pb}/^{206}\text{Pb}$ (left), and type B spectra, such as the second Pb principal component and ϵ_{Nd} (right), show peaks at the same wavelengths characteristic of each spectrum type. This suggests a similar long-wavelength structure.

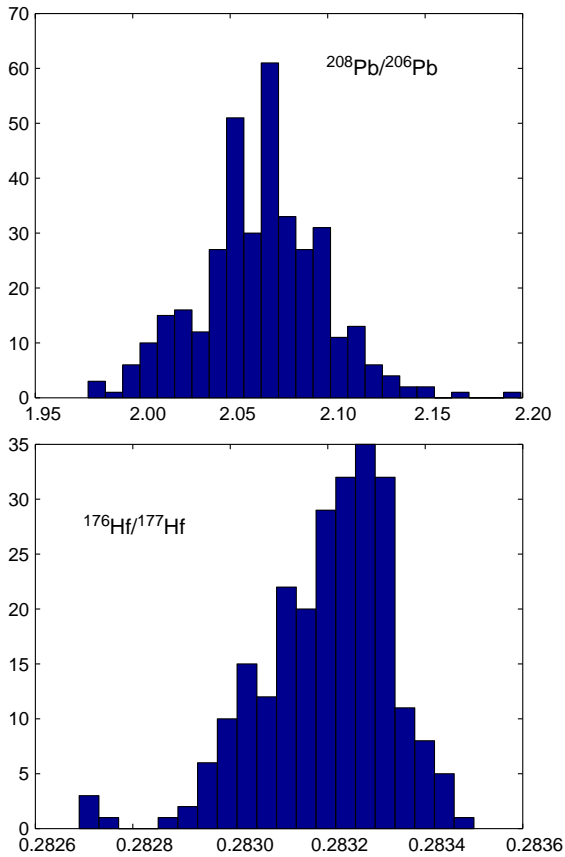


Fig. 7. Histograms of the $^{208}\text{Pb}/^{206}\text{Pb}$ and $^{176}\text{Hf}/^{177}\text{Hf}$ ratios used in this work. The histograms are strongly unimodal and show no evidence that a background of MORB with an asthenospheric signature is overprinted by hot spot material.

ent samples of arbitrary size will not record much deviation around a mean composition. A similar description would apply to delamination of the sub-continental lithosphere. Mathematically speaking, geochemical ‘variance’ is added at the long-wavelength end of the spectrum in the form of large anomalies, which in turn are progressively reduced in length scale and amplitude by the convective mantle flow and ultimately destroyed by diffusion. Variance therefore cascades down the wavenumber scale. For a given initial distribution of heterogeneities, it is now understood that both Lagrangian stretching and advective–diffusive transport end up producing time-dependent power law spectra [36,37], such as

$$P(k) \propto e^{-\gamma k} k^{-\sigma}$$

in which γ is a coefficient describing the rate of variance (i.e., heterogeneity) reduction and σ is the power law coefficient. Both coefficients depend on the flow regime and relate to the Lyapunov exponents of the flow field, which may simply be described as the maximum average rate of stretching experienced by a parcel of material following the flow. When new heterogeneities keep on being introduced, as is the case with subduction, the system is expected to relax from the initial conditions and evolve towards some sort of steady-state. Obtaining values for σ is considered important as they indicate whether mixing is dominated by the local properties of Lagrangian stretching [36] or by boundary conditions [37], i.e., in the present case, by the overall geometry of mantle convection.

The σ power law coefficient of type B spectra of the $^{143}\text{Nd}/^{144}\text{Nd}$, $^{176}\text{Hf}/^{177}\text{Hf}$, and second Pb principal component is, within error, about -1 (Fig. 5). A spectrum in k^{-1} is characteristic of the ‘Batchelor regime’ in which the length scale of momentum diffusive transport (viscosity) largely exceeds the length scale of chemical diffusion. It is the regime of tracer transport by smooth, but chaotic flow. It always dominates at steady-state, when variance of the tracer field is created at long wavelength (as effectively done in the mantle by plate subduction) and cascades in a linear way, i.e., with a variance flow proportional to the power of the variance at the same wavelength [38]. This contrasts with the $-5/3$ coefficient obtained by Metcalfe et al. [6] for the long-wavelength range of tracer distribution obtained in viscous chaotic flow experiments and which probably reflects either a transient regime or the effect of the periodic movement imposed by the walls of the fluid tank. This regime also differs from Allègre and Lewin’s [39] theory of mixing, in which conservation equations are applied to the standard deviation, an estimator of the dispersion which cannot easily be related to the power spectrum.

The overall north–south trend observed for type B spectra hints at some geochemical provinciality and likely reflects the southward increasing influence of the Dupal (Southern Hemisphere) anomaly [22,40,41]. Blichert-Toft et al. [12] and Debaille et al. (submitted) matched the second Pb principal component of their respective data sets with a mixture of the enriched geochemical end-members EM I and EM II (see also [42]), which are precisely the two geochemical end-members adding up to the Dupal signature. All obser-

vations therefore seem to imply that narrow streaks of Dupal mantle appear scattered all along the mid-Atlantic Ridge. As a unifying interpretation, we suggest that the spectra of isotopic anomalies along the mid-Atlantic Ridge depict how convection is ‘reeling off’ large regions of anomalous South Atlantic mantle. Plates refolded a number of times coalesce into regional anomalies the size of the African Superplume, now observed as a well-defined low-velocity region in the deep mantle [43], and into even larger mantle regions the size of the Dupal anomaly. Such plates may carry large oceanic plateaus, terrigenous sediments, perhaps even small continental fragments, which by themselves or together could be at the origin of the mixed EM I+EM II signature of the Dupal mantle [44,45]. Alternatively, delaminated lower continental crust [46,47] has been suggested to confer to large regions of the mantle the isotopic characteristics of the Southern Hemisphere anomaly. These broad regions must be sufficiently old to be hot and therefore seismically slow, but they also must be young enough to have survived shearing and dissemination by mantle convection. They relate indirectly to the long-wavelength hot spot contribution to the MORB spectra since ponding of such blobs at the base of the mantle provides fertile and hot sources for future hot spots. Mantle convection and plate subduction steadily plough the interface of these blobs, tearing off shreds and snippets of anomalous mantle that become stretched and refolded by the circulation and occasionally end up in the ridge system along the Central and Northern Atlantic.

We therefore suggest that, in addition to the effect of a small number of hot spots, the spectrum of isotopic heterogeneities along the mid-Atlantic Ridge reflects the convective dispersal of large-scale mantle anomalies. In the present case, the prominent Dupal anomalous mantle in the Southern Hemisphere seems to be the source of the short-wavelength variability observed in the Atlantic MORB. Such a mechanism predicts that, occasionally, Dupal isotopic signatures may occur far into the Northern Hemisphere.

3. Conclusions

New Pb, Hf, and Nd isotopic data on mid-Atlantic MORB have allowed us to produce spectra of isotopic heterogeneities along the entire mid-Atlantic Ridge.

Two contrasting types of spectra are observed. The first type (A) is common to $^{206}\text{Pb}/^{204}\text{Pb}$, $^{207}\text{Pb}/^{204}\text{Pb}$, $^{208}\text{Pb}/^{204}\text{Pb}$, the first Pb principal component, $^{87}\text{Sr}/^{86}\text{Sr}$, and $^3\text{He}/^4\text{He}$ and demonstrates the effect of hot spots at long wavelengths, while showing a white spectrum at short wavelengths. Type B spectra are common to $^{143}\text{Nd}/^{144}\text{Nd}$, $^{176}\text{Hf}/^{177}\text{Hf}$, and the second Pb principal component. They display a more continuous decrease with decreasing wavelength (cascade), indicative of a progressive reduction of the size of larger anomalies. The power law coefficient of the spectrum is characteristic of the Batchelor regime and reflects a smooth, but chaotic, probably steady-state flow. Since these isotopic properties are also characteristic of the EM I+EM II mix of the Dupal anomaly, we interpret the second type of spectrum as indicating the northward convective dispersal (‘reeling off’) of the Southern Hemisphere anomalous mantle.

Acknowledgements

We would like to thank, first and foremost, Jean-Guy Schilling for granting us access to one of the best MORB collections in the world and for being supportive of our efforts. We thank equally warmly Richard Kingsley for his precious and time-consuming help in sampling the MORB analyzed here from this collection. The Lithothèque Nationale in Brest also generously contributed some 30 samples. Discussions with Dan McKenzie and John Rudge helped clarify some of the thorny aspects of periodogram analysis and physics of fluids. Reviews by Bernard Bourdon, Vincent Salters, and Paul Tackley led to major changes and clarifications. Financial support by the DyETI program of Institut des Sciences de l’Univers (CNRS) is gratefully acknowledged. The steadfast help of Philippe Telouk with the Plasma 54 and Chantal Douchet in the clean laboratory is also much appreciated. DG was supported by the Marine Geology program of the National Science Foundation.

Appendix A. Supplementary Data

Supplementary data associated with this article can be found, in the online version, at [doi:10.1016/j.epsl.2005.07.011](https://doi.org/10.1016/j.epsl.2005.07.011).

References

- [1] E.M. Klein, C.H. Langmuir, Global correlations of ocean ridge basalt chemistry with axial depth and crustal thickness, *J. Geophys. Res.* 92 (1987) 8089–8115.
- [2] J.-G. Schilling, M. Zajac, R. Evans, T. Johnston, W. White, J.D. Devine, R. Kingsley, Petrologic and geochemical variations along the mid-Atlantic Ridge from 29°N to 73°N, *Am. J. Sci.* 283 (1983) 510–586.
- [3] U.R. Christensen, A.W. Hofmann, Segregation of subducted oceanic crust in the convecting mantle, *J. Geophys. Res.* 99 (1994) 19867–19884.
- [4] D. McKenzie, R.K. O’Nions, Mantle reservoirs and oceanic island basalts, *Nature* 301 (1983) 229–231.
- [5] C.J. Allègre, D.L. Turcotte, Implications of a two-component marble-cake mantle, *Nature* 323 (1986) 123–127.
- [6] G. Metcalfe, C.R. Bina, J.M. Ottino, Kinematic considerations for mantle mixing, *Geophys. Res. Lett.* 22 (1995) 743–746.
- [7] B. Hamelin, B. Duprè, C.J. Allègre, Lead-strontium isotopic variations along the East Pacific Rise and the mid-Atlantic Ridge, *Earth Planet. Sci. Lett.* 67 (1984) 340–350.
- [8] M. Gurnis, Quantitative bounds on the size-spectrum of isotopic heterogeneity within the mantle, *Nature* 323 (1986) 317–320.
- [9] D.W. Graham, F.J. Spera, Spatial statistics of isotopic variations along mid-ocean ridges, *J. Conf. Abst.* 5 (2000) 452.
- [10] F. Albarède, P. Télouk, J. Blichert-Toft, M. Boyet, A. Agranier, B. Nelson, Precise and accurate isotopic measurements using multiple-collector ICPMS, *Geochim. Cosmochim. Acta* 68 (12) (2004) 2725–2744.
- [11] J. Blichert-Toft, C. Chauvel, F. Albarède, Separation of Hf and Lu for high-precision isotope analysis of rock samples by magnetic sector-multiple collector ICP-MS, *Contrib. Mineral. Petrol.* 127 (1997) 248–260.
- [12] J. Blichert-Toft, A. Agranier, M. Andres, R. Kingsley, J.-G. Schilling, F. Albarède, Geochemical segmentation of the mid-Atlantic Ridge North of Iceland and ridge-hotspot interaction in the North Atlantic, *Geochem. Geophys. Geosyst.* 6 (2005), doi:10.1029/2004GC000788.
- [13] W.M. White, F. Albarède, P. Télouk, High-precision analysis of Pb isotopic ratios using multi-collector ICP-MS, *Chem. Geol.* 167 (2000) 257–327.
- [14] J. Douglass, J.-G. Schilling, D. Fontignie, Plume-ridge interactions of the Discovery and Shona mantle plumes with the southern mid-Atlantic Ridge (40°–55°S), *J. Geophys. Res.* 104 (1999) 2941–2962.
- [15] L. Dosso, B.B. Hanan, H. Bougault, J.-G. Schilling, J.-L. Joron, Sr–Nd–Pb geochemical morphology between 10°N and 17°N on the mid-Atlantic Ridge: a new MORB isotope signature, *Earth Planet. Sci. Lett.* 106 (1991) 29–43.
- [16] M.F. Thirlwall, M.A.M. Gee, R.N. Taylor, B.J. Murton, Mantle components in Iceland and adjacent ridges investigated using double-spike Pb isotope ratios, *Geochim. Cosmochim. Acta* 68 (2004) 361–386.
- [17] B.B. Hanan, D.W. Graham, Lead and helium isotope evidence from oceanic basalts for a common deep source of mantle plumes, *Science* 272 (1996) 991–995.
- [18] J.-G. Schilling, R.H. Kingsley, B.B. Hanan, B.L. McCully, Nd–Sr–Pb isotopic variations along the Gulf of Aden: evidence for Afar mantle plume–continental lithosphere interaction, *J. Geophys. Res.* 97 (1992) 10927–10966.
- [19] R.A. Johnson, D.W. Winchern, *Applied Multivariate Statistical Analysis*, Prentice-Hall, Englewood Cliff, 1992, 594 pp.
- [20] A.W. Hofmann, Mantle geochemistry: the message from oceanic volcanism, *Nature* 385 (1997) 219–229.
- [21] S.E. Church, M. Tatsumoto, Lead isotope relations in oceanic ridge basalts from the Juan de Fuca-Gorda Ridge area, NE Pacific Ocean, *Contrib. Mineral. Petrol.* 53 (1975) 253–279.
- [22] S.R. Hart, A large-scale isotope anomaly in the Southern Hemisphere mantle, *Nature* 309 (1984) 753–757.
- [23] A.W. Zindler, S.R. Hart, Chemical Geodynamics, *Annu. Rev. Earth Planet. Sci.* 14 (1986) 493–571.
- [24] D.W. Graham, Noble gas isotope geochemistry of mid-ocean ridge and ocean island basalts; characterization of mantle source reservoirs, in: D. Porcelli, R. Wieler, C. Ballentine (Eds.), *Noble Gases in Geochemistry and Cosmochemistry*, Rev. Mineral. Geochem., vol. 47, Mineral. Soc. Amer., Washington, D.C., 2002, pp. 247–318.
- [25] N.R. Lomb, Least-squares frequency analysis of unequally spaced data, *Astrophys. Space Sci.* 39 (1976) 447–462.
- [26] J.D. Scargle, Studies in astronomical time series analysis: II. Statistical aspects of spectral analysis of unevenly spaced data, *Astrophys. J.* 263 (1982) 835–853.
- [27] W.H. Press, B.P. Flannery, S.A. Teukolsky, W.T. Vetterling, *Numerical Recipes: The Art of Scientific Computing*, Cambridge University Press, Cambridge, 1992, 818 pp.
- [28] D.L. Turcotte, G. Schubert, *Geodynamics*, 2nd ed., Univ. Press, Cambridge, 2002, 456 pp.
- [29] J.-G. Schilling, R. Kingsley, D. Fontignie, R. Poreda, S. Xue, Dispersion of the Jan Mayen and Iceland mantle plumes in the Arctic: a He–Pb–Nd–Sr isotope tracer study of basalts from the Kolbeinsey, Mohns, and Knipovich Ridges, *J. Geophys. Res.* 104 (1999) 10543–10569.
- [30] P. Olson, D.A. Yuen, D. Balsiger, Mixing of passive heterogeneities by mantle convection, *J. Geophys. Res.* 89 (1984) 436–525.
- [31] N.R.A. Hoffman, D.P. McKenzie, The destruction of geochemical heterogeneities by differential fluid motions during mantle convection, *Geophys. J. R. Astron. Soc.* 1985 (1985) 163–206.
- [32] J.P. Morgan, W.J. Morgan, Two-stage melting and the geochemical evolution of the mantle: a recipe for mantle plumpudding, *Earth Planet. Sci. Lett.* 170 (1999) 215–239.
- [33] D. Bercovici, S.I. Karato, Whole-mantle convection and the transition-zone water filter, *Nature* 425 (2003) 39–44.
- [34] C.J. Hawkesworth, M.S.M. Mantovani, P.N. Taylor, Z. Palacz, Evidence from the Parana of south Brazil for a continental contribution to Dupal basalts, *Nature* 322 (1986) 356–359.
- [35] I. Vlastelic, D. Aslanian, L. Dosso, H. Bougault, J.L. Olivet, L. Geli, Large-scale chemical and thermal division of the Pacific mantle, *Nature* 399 (6734) (1999) 345–350.

- [36] T.M. Antonsen, Z. Fan, E. Ott, E. Garcia-Lopez, The role of chaotic orbits in the determination of power spectra of passive scalars, *Phys. Fluids* 8 (1996) 3094–3104.
- [37] D.R. Fereday, P.H. Haynes, Scalar decay in two-dimensional chaotic advection and Batchelor-regime turbulence, *Phys. Fluids* 16 (2004) 4359–4370.
- [38] T.M. Antonsen, E. Ott, Multifractal power spectra of passive scalars convected by chaotic fluid flows, *Phys. Rev., A* 44 (1991) 851–857.
- [39] C.J. Allègre, E. Lewin, Isotopic systems and stirring times of the earth's mantle, *Earth Planet. Sci. Lett.* 136 (1995) 629–646.
- [40] B. Dupré, C.J. Allègre, Pb–Sr isotope variation in Indian Ocean basalts and mixing phenomena, *Nature* 303 (1983) 142–146.
- [41] M. Andres, J. Blichert-Toft, J.-G. Schilling, Nature of the depleted upper mantle beneath the Atlantic: evidence from Hf isotopes in normal mid-ocean ridge basalts from 79°N to 55°S, *Earth Planet. Sci. Lett.* 225 (2004) 89–103.
- [42] S.B. Shirey, J.F. Bender, C.H. Langmuir, Three-component isotopic heterogeneity near the oceanographer transform, mid-Atlantic Ridge, *Nature* 325 (1987) 217–222.
- [43] D. Helmberger, S. Ni, L. Wen, J. Ritsema, Seismic evidence for ultra-velocity zones beneath Africa and eastern Atlantic, *J. Geophys. Res.* 105 (2000) 23865–23878.
- [44] D. Gasperini, J. Blichert-Toft, D. Bosch, A. Del Moro, P. Macera, P. Télouk, F. Albarède, Evidence from Sardinian basalt geochemistry for recycling of plume heads into the Earth's mantle, *Nature* 408 (2000) 701–704.
- [45] F. Albarède, R. van der Hilst, Zoned mantle convection, *Philos. Trans. R. Soc., A* 360 (2002) 2569–2592.
- [46] B.B. Hanan, J. Blichert-Toft, D.G. Pyle, D.M. Christie, Contrasting origins of the upper mantle MORB source as revealed by Hf and Pb isotopes from the Australian–Antarctic discordance, *Nature* 432 (2004) 91–94.
- [47] S. Escrig, F. Capmas, B. Dupre, C.J. Allegre, Osmium isotopic constraints on the nature of the DUPAL anomaly from Indian mid-ocean-ridge basalts, *Nature* 431 (7004) (2004) 59–63.